



## OPEN ACCESS

## EDITED BY

Jinghui Fang,  
Yellow Sea Fisheries Research Institute  
(CAFS), China

## REVIEWED BY

Zengling Ma,  
Wenzhou University, China  
Xiaoting Fu,  
Ocean University of China, China  
Biswarup Sen,  
Tianjin University, China

## \*CORRESPONDENCE

Dongdong Xu  
xudong0580@163.com  
Nianjun Xu  
xunianjun@nbu.edu.cn

## SPECIALTY SECTION

This article was submitted to  
Marine Fisheries, Aquaculture and  
Living Resources,  
a section of the journal  
Frontiers in Marine Science

RECEIVED 30 March 2022

ACCEPTED 13 July 2022

PUBLISHED 04 August 2022

## CITATION

Zhang Y, Xu D, Li T, Qiao L and Xu N  
(2022) Effects of large-scale  
*Sargassum fusiforme* culture on  
phytoplankton community structure  
and water quality.  
*Front. Mar. Sci.* 9:907726.  
doi: 10.3389/fmars.2022.907726

## COPYRIGHT

© 2022 Zhang, Xu, Li, Qiao and Xu. This  
is an open-access article distributed  
under the terms of the [Creative  
Commons Attribution License \(CC BY\)](#).  
The use, distribution or reproduction  
in other forums is permitted, provided  
the original author(s) and the  
copyright owner(s) are credited and  
that the original publication in this  
journal is cited, in accordance with  
accepted academic practice. No use,  
distribution or reproduction is  
permitted which does not comply with  
these terms.

# Effects of large-scale *Sargassum fusiforme* culture on phytoplankton community structure and water quality

Yurong Zhang<sup>1,2</sup>, Dongdong Xu<sup>1\*</sup>, Tiejun Li<sup>1</sup>, Ling Qiao<sup>1</sup>  
and Nianjun Xu<sup>2\*</sup>

<sup>1</sup>Key Lab of Mariculture and Enhancement of Zhejiang Province, Zhejiang Marine Fisheries Research Institute, Zhoushan, China, <sup>2</sup>Key Laboratory of Marine Biotechnology of Zhejiang Province, School of Marine Sciences, Ningbo University, Ningbo, China

The large-scale cultivation of *S. fusiforme* was hypothesized to effectively improve water quality and environmental characteristics. Specifically, such cultivation could promote habitat restoration effects by increasing DO and pH levels in addition to decreasing nitrogen and phosphorus levels within cultivation area waters. Phytoplankton diversity could also reflect the quality and health of waters. This study explored the effects of large-scale cultivation of *Sargassum fusiforme* on the biodiversity and the ecosystem of a phytoplankton community in the coastal waters of Dongtou island, China. *S. fusiforme* cultivation increased DO and pH values within the area but decreased N contents of the cultivation area waters. A total of 75 phytoplankton species were identified based on morphological identification, while a parallel survey of phytoplankton communities using high-throughput cultivation-independent sequencing identified 601 phytoplankton OTUs. Large scale cultivation of *S. fusiforme* was associated with increased phytoplankton diversity as reflected by multiple alpha and beta diversity metrics. These data suggested that *S. fusiforme* cultivation could affect phytoplankton community structure when the *S. fusiforme* biomass reached maximum levels. Redundancy analysis (RDA) indicated that *S. fusiforme* played an important role in controlling the dynamics of phytoplankton communities in coastal ecosystems. Thus, the results suggested that *S. fusiforme* cultivation could enhance phytoplankton community biodiversity. Overall, this study demonstrated that large-scale cultivation of *S. fusiforme* in coastal regions was an effective approach for mitigating environmental problems in marine ecosystems.

## KEYWORDS

*Sargassum fusiforme*, harmful algal blooms, phytoplankton biodiversity, high-throughput sequencing, bioremediation

# 1 Introduction

Phytoplankton are important primary producers in marine ecosystems (Behrenfeld et al., 2006; Jardillier et al., 2010), as they assimilate nutrients, fix inorganic carbon, and produce organic matter (Falkowski et al., 2000; Emerson, 2014). Biodiversity is essential for enhancing ecosystem productivity but is also critical for maintaining stability at the community and ecosystem levels in addition to maximizing the resource use and ecological efficiency that underpin ecosystem services (Chai et al., 2018). Species composition and phytoplankton community diversity are highly sensitive to changing environmental conditions and are affected by physical, chemical, biological, and climatic factor (Leblad et al., 2020; Liu et al., 2022). Thus, phytoplankton community diversity serves as an indicator of the influences from environmental factors and processes (Peng et al., 2021; Parsons et al., 2021). Consequently, these community characteristics can be used as ecological indicators to evaluate aquatic ecosystem health (Chai et al., 2018; Shan et al., 2019; Navas-Parejo et al., 2020; Zhou et al., 2021).

Marine phytoplankton biodiversity research has primarily focused on microscopic morphological observations (Lee et al., 2010). However, morphological approaches have limitations for identifying species (Massana, 2011), (Manoylov, 2014) for example in picophytoplankton that exhibit very small cell sizes or organisms that have no clear defining morphological characteristics in addition to those species that have not yet been described or characterized (Egge et al., 2015; de Vargas et al., 2015; Malviya et al., 2016; Liu S et al., 2020). Furthermore, high levels of impurities such as sediments in samples can lead to the inability to observe species. Moreover, morphological observation methods generally take considerable amounts of time and require specialist training for morphological identification. The rapid development of molecular biology tools has led to breakthroughs in understanding microalgae diversity (Lefebvre et al., 2005). Handelsman et al. (1998) formally proposed the field of metagenomics in 1998, focusing on understanding the diversity of microorganisms *via* environmental genomics techniques. Subsequent studies have demonstrated that high-throughput metagenomic sequencing methods are much more effective than morphological approaches for exploring the spatio-temporal dynamics of marine phytoplankton communities (Egge et al., 2015; de Vargas et al., 2015; Chai et al., 2018; Qiao et al., 2020). The 18S rDNA genes represent small ribosomal subunit genes that exist in all eukaryotes and that have both informational and functional roles within cells (Liu et al., 2017). The genes comprise nine variable regions, among which the V4 and V9 regions are widely used in eukaryotic biodiversity studies (Neefs et al., 1990). For example, Stoeck et al. (2010) demonstrated that the V4 region better distinguishes species with close genetic relationships. Moreover, diversity results based on the V4 region are more closely aligned with those from full-length 18S rDNA

sequences compared to the results using the V9 region (Pawlowski et al., 2011; Dunthorn et al., 2012), thereby rendering the V4 region of 18S rDNA genes an appropriate tool for phytoplankton identification (Liu et al., 2017).

*Sargassum fusiforme* is a species endemic to the temperate coastal areas of the northwestern Pacific region and is particularly abundant in coastal waters of China, Korea, and Japan (Li et al., 2019). *S. fusiforme* is an edible alga in China and is widely cultivated in southeastern coastal areas, the Yellow Sea, and the Bohai Sea (Hu et al., 2016; Zhang et al., 2021). Among these areas, the yield and quality are highest near the coast of Zhejiang province, and especially the coastal area of Dongtuo Island (Zhang et al., 2002). The alga has become one of the most important species for seaweed mariculture in China in recent years due to its high economic value and increasing consumer demand (Chen et al., 2018). In addition to providing food for human consumption (Zhang et al., 2020), the algae have also been used as a traditional Chinese medicinal plant to treat various diseases (Zhang et al., 2006; Liu J et al., 2020).

Local farmers culturing *S. fusiforme* have observed that during *S. fusiforme* culture, and especially in April when *S. fusiforme* biomass is highest, red tides rarely occur in cultivation areas, while red tides frequently occur in the cultivation areas after the *S. fusiforme* harvest (local fisherman's expertis). Previous studies have shown that *S. fusiforme* can also inhibit *Karenia mikimotoi* growth (Ma et al., 2017). Interestingly, identification of microscopically observable microalgae has indicated that the abundance of one of the red tide microalgae, *Skeletonema costatum*, was significantly lower in the *S. fusiforme* cultivation areas compared to areas without *S. fusiforme* (unpublished data). These observations prompted the present study to evaluate whether a positive impact on phytoplankton community diversity occurs due to *S. fusiforme* cultivation, and also whether the latter influences the cell abundances of red tide microalgae. Moreover, these studies were used to evaluate whether additional red tide microalgae could be inhibited by *S. fusiforme*. To investigate these hypotheses, we analyzed the phytoplankton biodiversity associated with *S. fusiforme* cultivation *via* high-throughput sequencing of 18S rRNA genes using newly designed PCR primers for eukaryotes. In addition, water quality parameters in *S. fusiforme* cultivation and non-cultivation areas were analyzed in tandem. These results are of significance for comprehensively understanding the ecological value of large-scale *S. fusiforme* culture.

## 2 Materials and methods

### 2.1 Sampling site descriptions

The study area is located at the Banpingshan cultivation zone in southeastern Dongtuo Island (27°41'19"–28°01'10" E,

120°59'45"–121°15'58" N), one of the largest *S. fusiforme* mariculture bases in the Dongtou district (Figure 1). The cultivation area was only 57.2 ha in 1989 and is currently maintained at approximately 1,000 ha per year, with an annual seaweed dry-weight production of about 7,000–9,000 tons.

In total, 54 samples were collected in April and June 2019. Nine sampling sites were selected in areas with and without *S. fusiforme* cultivation. The sampling sites and samples were collected as follows: (1) A: *S. fusiforme* cultivation areas, comprising three sites (A1–A3), (2) B: 200–500 m away from the “A” cultivation areas, with three sites (B1–B3), and C: three sites in the open sea about 2 km away from the cultivation area (C1–C3). The average depths at sites A, B, and C were 9.0 m, 8.7 m, and 9.1 m, respectively. A total of 54 samples comprising three replicates for each site were collected from surface waters (0.5 m below the surface), with samples labeled as Ban Pingshan, BS, and CS. Samples were also identified by the time of sampling, with Apr-A, Apr-B, and Apr-C for April samples, and Jun-A, Jun-B and Jun-C for June samples.

## 2.2 Sample collection and water quality

Water samples (4 L) from the surface and bottom of the sea were collected with organic glass hydrophores. A subsample (1 L) of water from each sample was then used for microbial community investigation by filtering with a sterile microfiltration membrane (47 mm, 0.22 μm filter). After filtering, microfiltration membranes were placed in 5 mL sterile tubes and immediately placed on dry ice.

The remaining water from each sample was stored at –80°C and transported to the laboratory. Dissolved oxygen (DO), salinity (Sal), temperature (T), and pH were measured for each

sample using 550A, EC300A, and PH100A YSI instruments, respectively (YSI Inc., Yellow Springs, OH, USA). Ammonia-nitrogen (NH<sub>4</sub><sup>+</sup>-N), nitrite-nitrogen (NO<sub>2</sub><sup>-</sup>-N), nitrate-nitrogen (NO<sub>3</sub><sup>-</sup>-N), active phosphate (PO<sub>4</sub><sup>3-</sup>-P), silicate (SiO<sub>3</sub><sup>2-</sup>), total nitrogen (TN), and total phosphorus (TP) were all measured using previously described methods (Zhang et al., 2021).

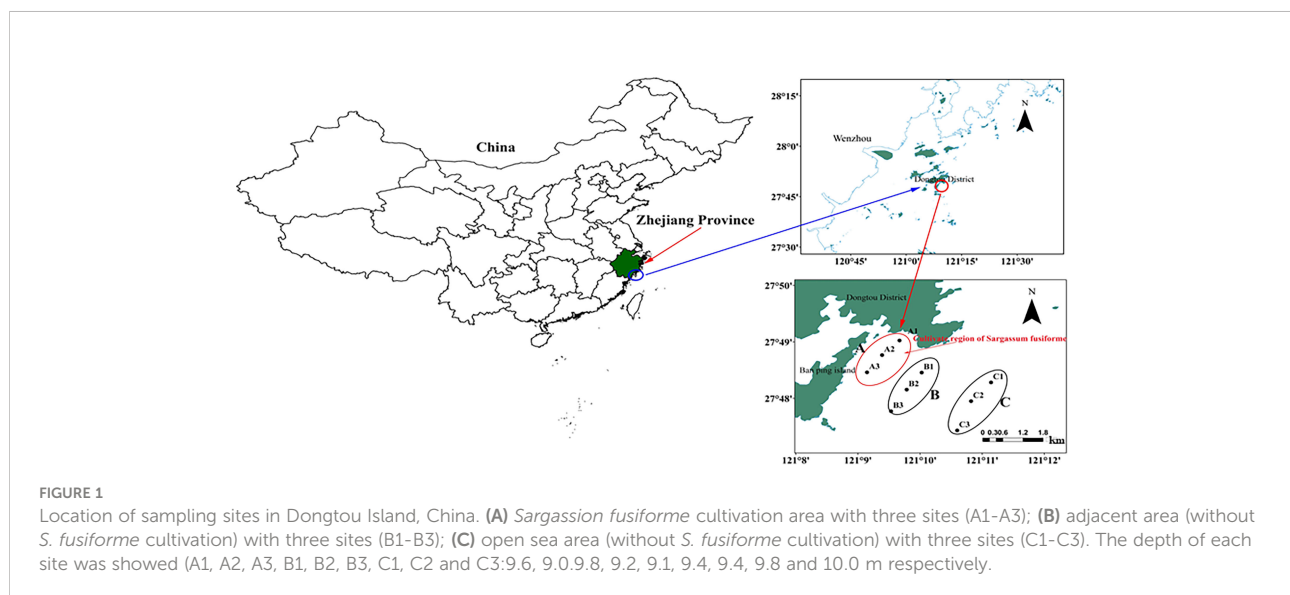
## 2.3 Phytoplankton morphological analyses

Unfiltered water samples (1 L) were fixed with 5 mL of Lugol's solution, and each sample was subsequently concentrated to 10 mL. Phytoplankton species were identified in these samples, and cell numbers were counted using a phytoplankton enumeration chamber with an inverted microscope (Olympus CKX41, Olympus Corporation, Tokyo, Japan).

## 2.4 High-throughput sequencing of phytoplankton and bioinformatics analyses

### 2.4.1 DNA extraction, PCR amplification, and sequencing

Total genomic DNA was extracted from samples using the FastDNA spin kit for soils (MP Biomedicals, OH, USA), following the manufacturer's instructions. DNA quality and concentration were measured by gel electrophoresis and a Nanodrop spectrophotometer (NanoDrop Technologies, Wilmington, DE, USA), respectively. PCR was performed using the 18S rDNA gene primer pair 18sV4F (5'-CCAGCASCYCGGGTAATTCC-3') and 18sV4R (5'-



ACTTTCGTTCTTGATYRA-3' (Stoeck et al., 2010). PCR products were extracted from a 2% agarose gel and further purified using the AxyPrepDNA Gel Extraction Kit (Axygen Biosciences, USA) according to the manufacturer's instructions, and then quantified using the QuantiFluor™-ST system (Promega, USA). Purified amplicons were pooled in equimolar concentrations and subjected to paired-end (PE300) read sequencing on an Illumina MiSeq platform (Illumina, San Diego, USA) at Majorbio Bio-Pharm Technology Co. Ltd. using standard protocols (Shanghai, China). Sequence data were deposited in GenBank under the accession number PRJNA761497.

### 2.4.2 Bioinformatic analysis

The pretreatment of raw data was performed by QIIME software (Caporaso et al., 2010). The raw tags were merged by FLASH using an overlap length > 10 bp and a maximum mismatch rate < 0.2. The quality filtration of raw tags was executed by Trimmomatic software, and raw tags with a quality level < 75% were discarded. The UCHIME software was applied to identify and discard the chimeric sequences. The valid tags were clustered into operational taxonomic units (OTUs) at a 97% identify threshold. The OTUs were annotated and classified by QIIME software based on the Silva database. Taxonomic assignments were determined for representative sequences of each OTU using the Basic Local Alignment Search Tool (BLAST) in the NCBI database (<http://www.ncbi.nlm.nih.gov>). Following the exclusion of sequences annotated as bacterial and those that were unclassified, phytoplankton sequences were selected for community compositional analyses based on taxonomic information.

### 2.4.3 Ecological network analysis of the microbial community

To illuminate phytoplankton interactions and differences between groups, phylogenetic molecular ecological networks (pMENs) were constructed *via* a random matrix theory-based interface approach in the molecular ecological network analysis pipeline (MENA, <http://ieg2.ou.edu/MENA/>)

## 2.5 Phytoplankton community analysis

The dominance of abundant species identified by morphological analysis (> 10% of communities) was defined as the species cell abundance/total cell abundance ratio. The dominance of abundant genera revealed by high-throughput sequencing (>10% of sequence reads) was defined as the percentage of sequences for the taxa among the total sequences. Phytoplankton were further classified as picophytoplankton ( $\leq 2 \mu\text{m}$ ), small nanophytoplankton ( $> 2 \mu\text{m}$  and  $\leq 10 \mu\text{m}$ ), large nanophytoplankton ( $> 10 \mu\text{m}$  and  $< 20$

$\mu\text{m}$ ), and microphytoplankton ( $> 20 \mu\text{m}$  and  $< 200 \mu\text{m}$ ) based on cell sizes (Qiao et al., 2020).

Three  $\alpha$ -diversity metrics were calculated for communities, the Shannon–Wiener, Simpson, and Ace indices, using the QIIME software program. Differences in  $\alpha$ -diversity metric values were analyzed by one-way ANOVA, and statistical analyses were performed with the SPSS software program (v. 22.0). Prior to statistical analyses, data were checked for normality of distributions and homogeneity of variance by the Kolmogorov-Smirnov and Levene's tests, respectively. Statistical significance was identified at the  $p < 0.05$  level.  $\beta$ -diversity was also calculated as a comparative indicator of community structures among samples. Histograms of phyla and classes were constructed using the Origin 9.0 software program. In addition, linear model-based redundancy analysis (RDA) was used based on correlations among phytoplankton community composition and water quality parameters with the Canoco 5.0 software package.

## 3 Results

### 3.1 Water quality parameters

*S. fusiforme* cultivation increased DO and pH values but decreased N contents of the cultivation area waters. The DO,  $\text{NO}_3\text{-N}$ ,  $\text{NO}_2\text{-N}$ , and TN values of the cultivation area in April 2019 were significantly higher than in the adjacent and control areas ( $p < 0.05$ ). In June 2019,  $\text{NO}_3\text{-N}$  was significantly higher in the cultivation area than in the adjacent and control areas.  $\text{NO}_2\text{-N}$  and  $\text{NH}_4\text{-N}$  were also significantly higher in the cultivation area than in the control area ( $p < 0.05$ ) (Table 1).

### 3.2 Phytoplankton community composition

Five phyla 75 species of phytoplankton were observed based on morphological observations: Bacillariophyta, Dinophyta, Chrysophyta, Cyanophyta, and Chlorophyta, with Bacillariophyta and Dinophyta being the most dominant phyla. The abundances of each phylum among different survey areas/times were as follows: Bacillariophyta (Apr-A=93.87%; Apr-B=94.15%; Apr-C=96.59%; Jun\_A=94.94%; Jun\_B=88.71%; Jun\_C=88.58%), Dinophyta (Apr-A=1.82%; Apr-B=2.85%; Apr-C=1.01%; Jun\_A=4.16%; Jun\_B=9.72%; Jun\_C=9.72%), Chrysophyta (Apr-A=1.82%; Apr-B=1.00%; Apr-C=0.71%; Jun\_A=0.00%; Jun\_B=0.52%; Jun\_C=0.33%), Cyanophyta (Apr-A=1.21%; Apr-B=1.00%; Apr-C=0.74%; Jun\_A=0.44%; Jun\_B=0.52%; Jun\_C=0.33%), and Chlorophyta (Apr-A=1.28%; Apr-B=1.00%; Apr-C=1.01%; Jun\_A=0.46%; Jun\_B=0.52%; Jun\_C=0.33%) (Figure 2A).

TABLE 1 Temporal and spatial variation in environmental parameters of waters measured in 2019.

Parameter	April			June		
	AS	BS	CS	AS	BS	CS
Depth (m)	10.0±0.24	9.9±0.27	9.9±0.15	10.0±0.18	9.8±0.21	10.0±0.13
Temperature (°C)	14.6±0.2	14.7±0.2	14.5±0.2	22.0±0.4	22.1±0.1	22.3±0.1
Salinity	26.5±0.2	26.5±0.1	26.5±0.1	28.2±0.2	28.4±0.1	28.3±0.0
pH	8.32±0.05	8.21±0.02	8.13±0.03*	8.23±0.0	8.25±0.0	8.27±0.0
DO (mg/L)	10.4±0.2	10.1±0.1*	10.1±0.1*	9.3±0.1	9.3±0.1	9.3±0.1
NO <sub>3</sub> -N (mg/L)	0.474±0.025	0.467±0.011	0.507±0.032*	0.317±0.109	0.287±0.008*	0.290±0.015*
NO <sub>2</sub> -N (mg/L)	0.008±0.008	0.009±0.008	0.026±0.017**	0.013±0.002	0.010±0.004	0.009±0.003*
NH <sub>4</sub> -N (mg/L)	0.149±0.019	0.133±0.018	0.121±0.024	0.102±0.027	0.095±0.003	0.093±0.003*
TN (mg/L)	3.12±0.35	3.07±0.26	3.33±0.36*	4.84±1.40	4.81±0.57	4.75±1.41
PO <sub>4</sub> -P (mg/L)	0.039±0.008	0.036±0.002	0.037±0.003	0.048±0.003	0.042±0.010	0.046±0.003
TP (mg/L)	0.05±0.01	0.05±0.01	0.05±0.01	0.041±0.01	0.042±0.01	0.040±0.01
SiO <sub>3</sub> -Si (mg/L)	0.452±0.027	0.445±0.445	0.447±0.036	0.720±0.026	0.717±0.004	0.720±0.031

Values are means ± standard deviations. \*: p < 0.05 indicating that BS or CS was significantly different from AS, based on one-way ANOVA t test. \*\*p < 0.01.

After removing macroalgal, zooplankton, protozoan, fungal, and unclassified OTUs from the sequence dataset *via* comparisons against the NCBI database and literature searches, a total of 601 phytoplankton OTUs were identified comprising the seven phyla Dinophyta, Bacillariophyta, Chlorophyta, Cryptophyta, Chrysophyta, Ochrophyta, and Rhodophyta. Among these, Bacillariophyta, Dinophyta, Chlorophyta, and Cryptophyta were the dominant phyla. The relative abundances of each phylum among the survey areas based on molecular analysis were as follows: Bacillariophyta (Apr-A=11.3%; Apr-B=13.6%; Apr-C=9.2%; Jun\_A=47.0%; Jun\_B=44.5%; Jun\_C=41.1%), Dinophyta (Apr-A=29.5%; Apr-B=32.0%; Apr-C=29.7%; Jun\_A=18.8%; Jun\_B=22.5%; Jun\_C=26.9%), Chlorophyta (Apr-A=32.8%; Apr-B=28.9%; Apr-C=31.2%; Jun\_A=23.0%; Jun\_B=19.3%; Jun\_C=18.8%), Cryptophyta (Apr-A=24.0%; Apr-B=22.7%; Apr-C=27.9%; Jun\_A=10.3%; Jun\_B=12.9%; Jun\_C=10.3%), Chrysophyta (Apr-A=1.0%; Apr-B=0.9%; Apr-C=0.8%; Jun\_A=0.7%;

Jun\_B=0.3%; Jun\_C=0.5%), Ochrophyta (Apr-A=1.2%; Apr-B=1.4%; Apr-C=1.1%; Jun\_A=0.2%; Jun\_B=0.4%; Jun\_C=0.4%), and Rhodophyta (Apr-A=0.2%; Apr-B=0.4%; Apr-C=0.1%; Jun\_A=0.0%; Jun\_B=0.0%; Jun\_C=0.0%) (Figure 2B).

Significant differences were observed for phytoplankton composition, specifically the abundances of Bacillariophyta, Ochlorophyta, Chlorophyta, Cryptophyta, and Rhodophyta between April and June communities (*p* < 0.05) (Figure 3). No significant differences were observed between Dinophyta and Chrysophyta abundances across the two time periods (*p* > 0.05). Bacillariophyta abundances in April were significantly higher than in June, while the abundances of Ochlorophyta, Chlorophyta, Cryptophyta, and Rhodophyta were significantly lower in April than in June.

A total of 23 genera/species of picophytoplankton and 17 genera/species of small nanophytoplankton were detected *via* high-throughput sequencing that were not observed with

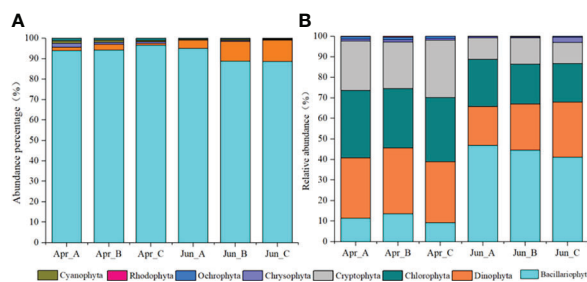


FIGURE 2 Temporal variation in the relative abundances of phytoplankton phyla based on morphological observations (A) and high-throughput sequencing (B) approaches.

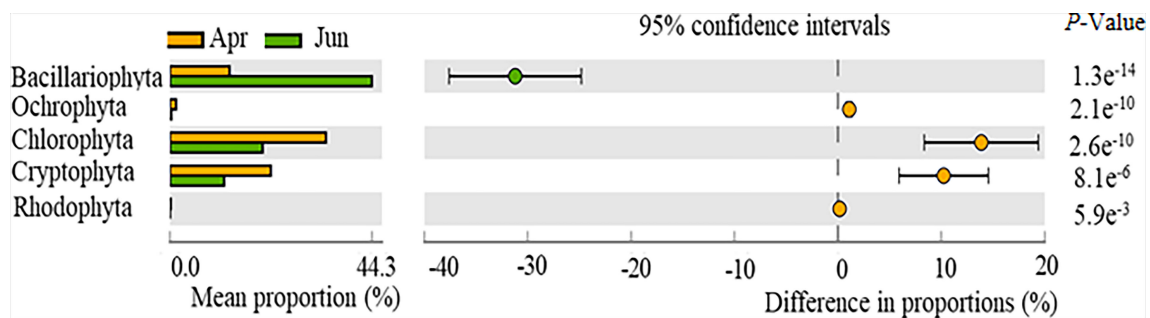


FIGURE 3 Temporal variation in the relative abundances of phytoplankton phyla, as observed with high-throughput sequencing of community compositions.

morphological analyses (Table 2), accounting for 22.21% and 13.18% of the abundance percentage. The dominant Chlorophyta species that were observed included *Bathycoccus prasinos*, *Micromonas pusilla*, *Pyramimonas australis*, and *Nannochloris* sp., all of which exhibited cell sizes less than 2  $\mu\text{m}$ ; all are considered to be photosynthetic picoeukaryotes (PPEs) and are widely distributed in marine environments (Mayer and Taylo, 1979; Luis et al., 1992; Rashid et al., 2018). Thus, the overall diversity and community structure of phytoplankton were not comprehensively evaluated by traditional morphological observations alone.

A total of 75 phytoplankton species were identified based on morphological characters, while a parallel survey of phytoplankton communities using high-throughput cultivation-independent sequencing identified 601 phytoplankton OTUs. Thus, the number of OTUs in this study was 3 to 7.6 times higher than the number of morphospecies identified from the same communities. Therefore, the high-throughput sequencing results were selected to analyze the dominant species and diversity of phytoplankton.

### 3.3 Dominant phytoplankton species or genera based on high-throughput sequencing

Dominant phytoplankton genera/species (dominance  $\geq 0.01$ ) were calculated based on OTU compositions. The dominant phytoplankton species were primarily distributed among the phyla Chlorophyta (6 OTUs), Cryptophyta (7 OTUs), Dinophyta (3 OTUs), and Bacillariophyta (10 OTUs). Among April communities, *Heterocapsa* sp. (Dinophyta) were dominant, with values in the cultivation, adjacent, and control areas of 0.165, 0.159, and 0.171, respectively. The second most dominant species was *Plagioselmis prolonga* (Cryptophylum) that exhibited dominance values of 0.109, 0.102, and 0.114, respectively, in the above areas. The third most abundant species was *B. prasinos* (Chlorophyta), with dominance values

of 0.086, 0.087, and 0.092, respectively. Among June communities, the most abundant species was *Heterocapsa* sp. (Dinophyta), with dominance values in the culture, adjacent, and control areas of 0.089, 0.080, and 0.076, respectively. The second most abundant species in June was *S. costatum* (Bacillariophyta), with dominance values of 0.092, 0.081, and 0.070 respectively. The third most abundant species was *Chaetoceros tenuissimus* (Bacillariophyta) that exhibited dominance values of 0.086, 0.074, and 0.080 respectively (Table 3).

Several dominant microalgae in the April communities, including *B. prasinos*, *Geminigera cryophila*, *Heterocapsa* sp., *S. marinoi*, and *Thalassiosira tenera*, exhibited lower dominance values in the adjacent and control areas. In June, *B. prasinos*, *G. cryophila*, *Heterocapsa* sp., *S. costatum*, and *T. tenera* exhibited higher dominance values in the cultivation area waters than in the adjacent or control areas. We consequently speculated that *S. fusiforme* exhibited an inhibitory effect on the above dominant species and that *S. fusiforme* selectively prevents the growth of some microalgae (Table 3).

### 3.4 Phytoplankton community structure based on high-throughput sequencing

#### 3.4.1 Phytoplankton community alpha diversity

Large scale cultivation of *S. fusiforme* was associated with increased phytoplankton diversity. Specifically, the Shannon-Wiener index of April communities in the culture area ( $3.29 \pm 0.15$ ) was significantly higher than in the control area ( $2.69 \pm 0.24$ ) ( $p < 0.05$ ). In contrast, no significant differences were observed among diversity values in June in the culture, adjacent, or control areas. The Simpson index values of the cultivation area communities in April ( $0.069 \pm 0.016$ ) were significantly lower than in the control area ( $0.088 \pm 0.005$ ) ( $p < 0.05$ ). In contrast, June culture area community Simpson index values ( $0.0980 \pm 0.026$ ) were significantly higher than in the adjacent ( $0.067 \pm 0.004$ ) ( $p < 0.05$ ) and control ( $0.063 \pm 0.006$ ) ( $p < 0.01$ )

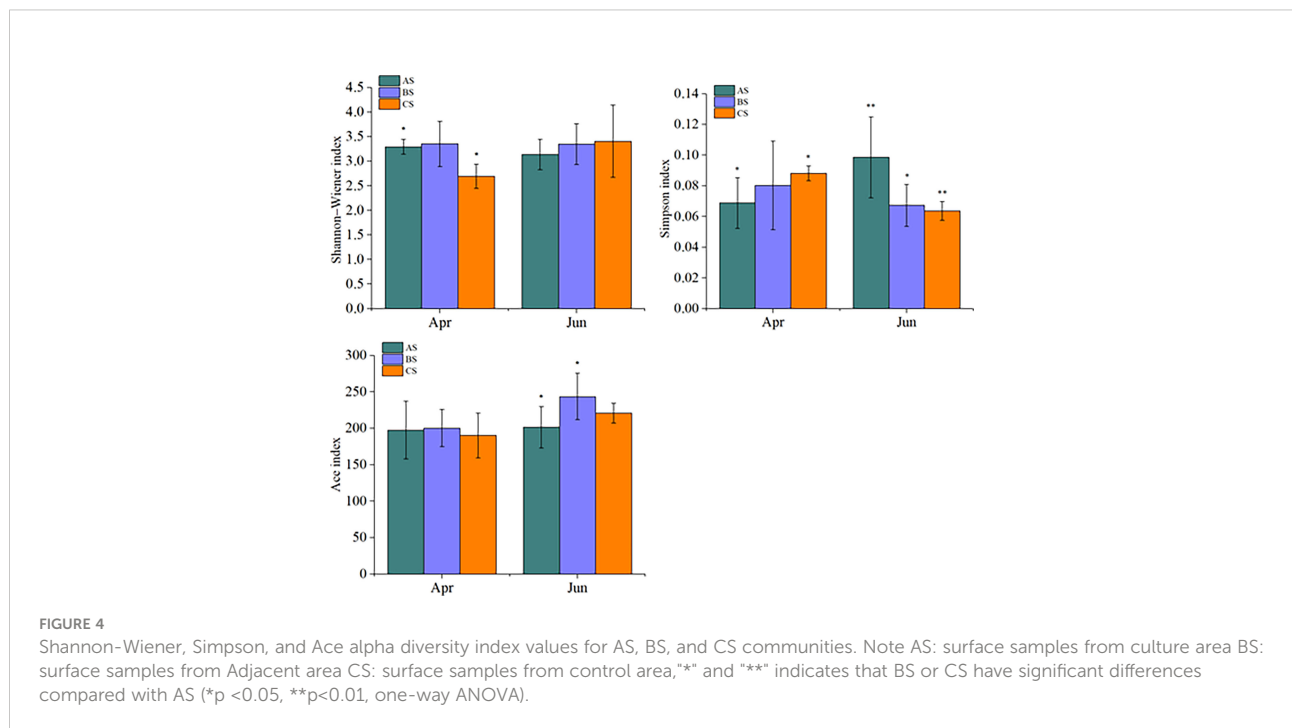
TABLE 2 List of described picophytoplankton and small nanophytoplankton species revealed by high-throughput sequencing.

Phylum	Genus	Closest known species	NCBI accession(similarity)	Relative abundance (%)	Cell size( $\mu\text{m}$ )	Reference
Picophytoplankton(Minimum size $\leq 2\mu\text{m}$ )						
Bacillariophyta	<i>Skeletonema</i>	<i>S. menzellii</i>	AB948147.1(99.74%)	0.72	2-12	(Pfannkuchen et al, 2018)
	<i>Skeletonema</i>	<i>S. marinoi</i>	KY364698.1(100%)	1.31	2-12	(Pfannkuchen et al, 2018)
	<i>Skeletonema</i>	<i>S. costatum</i>	KY290715 (94.50%)	4.78	2-12	(Pfannkuchen et al, 2018)
	<i>Skeletonema</i>	<i>S. potamos</i>	MW541631(91.88%)	0.00	2-12	(Pfannkuchen et al, 2018)
	<i>Skeletonema</i>	<i>S. subsalsum</i>	AY684967.1 (91.36%)	0.00	2-12	(Pfannkuchen et al, 2018)
	<i>Arcocellulus</i>	<i>A. cornucervi</i>	KU561153.1(100%)	0.21	1.0-17.0	(Vaulot et al., 2008)
	<i>Triparma</i>	<i>T. strigata</i>	KR998402.1(100%)	0.00	2.0-3.0	(Ichinomiya et al., 2019)
	<i>Brockmanniella</i>	<i>B.brockmannii</i>	KY979974 (100%)	0.02	2 $\times$ 10	(Samanta et al., 2017)
	<i>Chaetoceros</i>	<i>C.socialis</i>	KY852277.1(100%)	0.00	2 $\times$ 10	(Mahadik et al., 2017; Antoni et al., 2020)
Chlorophyta	<i>Micromonas</i>	<i>M. pusilla</i>	KY980039.1(100%)	4.83	0.2-0.3	(Song et al., 2020)
	<i>Bathycoccus</i>	<i>B. prasinos</i>	MT571465.1(100%)	5.35	1-3	(Simon et al., 2017)
	<i>Ostreococcus</i>	<i>Ostreococcus</i> sp.	MT117941(100%)	2.02	1-3	(Chai et al., 2018)
	<i>Micromonas</i>	<i>M.commoda</i>	KU612123.1(100%)	0.00	1.0-2.0	(Simon et al., 2017)
	<i>Pycnococcus</i>	<i>P.provasolii</i>	MK541772.1(100%)	0.00	$\leq 2\mu\text{m}$	(Moro et al., 2002)
	<i>Pyramimonas</i>	<i>P.tetrarhynchus</i>	FN562441.1(99.74%)	0.00	$\leq 2\mu\text{m}$	(Zhang et al., 2015)
	<i>Ostreococcus</i>	<i>Ostreococcus</i> sp.	JN862919.1(99.73%)	0.00	0.8	(Liu et al., 2017)
	<i>Nannochloris</i>	<i>Nannochloris</i> sp.	AB058312.1(100%)	2.84	2-4	(Qiao et al., 2020)
	<i>prasinophyte</i>	<i>prasinophyte</i> sp.	AB058375.1(100%)	0.00	2-5	(Jouenne et al., 2011)
	<i>Nannochloropsis</i>	<i>N. oculata</i>	KY054986.1(99.21%)	0.02	2-4	(Kagan and Matulka 2015)
	<i>Picochlorum</i>	<i>P.maculatum</i>	KM055115.1(99.21%)	0.00	1-2	(Augustine et al., 2017)
	<i>Stichococcus</i>	<i>S.bacillaris</i>	MT053478.1(100%)	0.01	2-3	(Sivakumar et al., 2014)
	<i>Tetrastrum</i>	<i>T.staurogeniiforme</i>	LC425390.1(99.74%)	0.00	2-5	(Bock et al., 2013)
	Ochrophyta	<i>Aureococcus</i>	<i>A.anophagefferen</i>	KY980028.1(100%)	0.00	1.5-2
small nanophytoplankton ( $\leq 10\mu\text{m}$ )						
Bacillariophyta	<i>Micrometopion</i>	<i>M.nutans</i>	HQ121441.1(92.03%)	0.00	5-7	(Howe et al., 2011)
	<i>Cyclotella</i>	<i>C.choctawhatcheana</i>	JQ217341.1(100%)	1.06	10	(Christiane, 2003)
	<i>Chaetoceros</i>	<i>C.muellerii</i>	JF790991.1(98.67%)	0.03	3.5-9.2	(Song et al., 2020)
	<i>Chaetoceros</i>	<i>C.calcitrans</i>	AY625894.1(100%)	0.10	2.8-3.0	(Song et al., 2020)
	<i>Mimodiscus</i>	<i>M. comicus</i>	MW722948.1(100%)	0.05	2.0-7.5	(Leblanc et al., 2018)
	<i>Chaetoceros</i>	<i>C.tenuissimus</i>	KC309487.1(99.74%)	0.04	5.0	(Tomaru et al., 2018)
	Cryptophyta	<i>Teleaulax</i>	<i>T.amphioxoia</i>	KY980249 (100%)	8.31	5.0-6.8
<i>Goniomonas</i>		<i>G.avonlea</i>	JQ434475.1(90.31%)	0.02	9.7	(Song et al., 2020)
<i>Plagioselmis</i>		<i>prolonga</i>	MK956143.1(100%)	0.11	(5-7) $\times$ (3-3.7)	(Xing et al., 2008)
Chlorophyta	<i>Dolichomastix</i>	<i>Dolichomastix</i> sp.	FN562449.1(96.32%)	0.02	3.0-5.0	(Vaulot et al., 2008)
	<i>Prasinoderma</i>	<i>Prasinoderma</i> sp.	AB058379.1(94.01%)	0.00	2.2-5.5	(Vaulot et al., 2008)
Ochrophyta	<i>Florenciella</i>	<i>Florenciella</i> sp.	AB518483.1(99.74%)	0.01	3.0-6.0	(Vaulot et al., 2008)
	<i>Pseudochattonella</i>	<i>P.verruculosa</i>	AB217629.1(99.74%)	0.03	5 $\times$ 10	(Lincoln et al., 2011)
	<i>Ciliophrys</i>	<i>C.infusionum</i>	AB081641.1(89.41%)	0.00	5	(Hiroshi et al., 2002)
Chlorophyta	<i>Tetraselmis</i>	<i>Tetraselmis</i> sp.	MH055454 (98.95%)	0.73	(8-16) $\times$ (7-9) $\times$ (3-5)	(Nozaki, 2003)
	<i>Pyramimona</i>	<i>P.australis</i>	KY980350.1(100%)	2.71	8	(Moro et al., 2002)
	<i>Mamiella</i>	<i>M.gilva</i>	FN562450.1(99.47)	0.12	(5-8) $\times$ (4-7)	(Alonso-González et al., 2014)

**TABLE 3** Dominant genera and species based on high throughput sequencing, in addition to their dominance values and sequence similarity to database accessions.

Phylum	Taxa	OTU ID	April				June				NCBIAccession (similarity)
			AS	BS	CS	All	AS	BS	CS	All	
Chlorophyta	s: <i>Bathycoccus prasinos</i>	OTU1583	0.086	0.087	0.092	0.088	0.019	0.014	0.015	0.016	MT571465.1 (100%)
	g: <i>Ostreococcus</i> sp.	OTU99	0.043	0.046	0.033	0.041	/	/	/		MT117941 (100%)
	s: <i>Micromonas pusilla</i>	OTU2003	0.036	0.035	0.044	0.038	0.076	0.049	0.054	0.060	KT860879.1 (100%)
	g: <i>Micromonas</i> sp.	OTU557	0.034	0.033	0.032	0.033	/	/	/		MT117944.1 (100%)
	s: <i>Pyramimonas australis</i>	OTU1951	0.030	0.027	0.027	0.028	0.034	0.025	0.021	0.027	KY980350.1 (100%)
	g: <i>Picochlorum</i> sp.	OTU3226	0.041	0.022	0.021	0.028	0.027	0.030	0.025	0.027	KT860896.1 (100%)
Cryptophyta	g: <i>Plagioselmis prolonga</i>	OTU350	0.109	0.102	0.114	0.108	0.020	0.020	0.020	0.020	MK956143.1 (100%)
	g: <i>Teleaulax gracilis</i>	OTU1747	0.030	0.036	0.033	0.033	0.016	0.024	0.022	0.021	JQ966995 (98.93%)
	s: <i>Storeatula major</i>	OTU232	0.018	0.015	0.017	0.016	0.020	0.020	/	0.020	KY980340.1 (100%)
	s: <i>Teleaulax minuta</i>	OTU3028	/	/	/		0.014	0.015	0.016	0.015	JQ966996.1 (99.73%)
	s: <i>Geminigera cryophila</i>	OTU489	0.015	0.017	0.015	0.016	0.023	0.024	0.022	0.023	MK956818.1 (98.93)
Dinophyta	g: <i>Heterocapsa</i> sp.	OTU1048	0.165	0.159	0.171	0.165	0.089	0.080	0.076	0.082	MH071708.1 (99.74)
	s: <i>Heterocapsa rotundata</i>	OTU2153	0.040	0.046	0.049	0.045	0.027	0.039	0.045	0.037	KY980288 (100%)
	g: <i>Warnowia</i> sp.	OTU667	0.057	0.072	0.063	0.064	0.018	0.022	0.031	0.024	KY980035.1 (100%)
Bacillariophyta	s: <i>Skeletonema marinoi</i>	OTU1132	0.016	0.023	0.014	0.018	/	/	/	/	KY364698.1 (100%)
	s: <i>Skeletonema costatum</i>	OTU1820	/	/	/	/	0.092	0.081	0.070		KY290715 (94.50%)
	s: <i>Thalassiosira rotula</i>	OTU2063	0.010	0.010	0.010	0.010	/	/	/	/	KT860983.1 (99.22%)
	s: <i>Thalassiosira tenera</i>	OTU601	0.048	0.054	0.027	0.043	0.041	0.048	0.041	0.043	MW722948.1 (100%)
	g: <i>Minidiscus comicus</i>	OTU1983	0.010	/	0.068	0.039	0.076	0.072	0.023	0.057	MN528623.1 (100%)
	s: <i>Cerataulina pelagica</i>	OTU2032	/	/	/	/	0.020	/	0.030	0.025	KC309487.1 (99.74%)
	g: <i>Chaetoceros</i> sp.	OTU2669	/	/	/	/	0.086	0.074	0.080	0.080	MG972315.1 (100%)
	s: <i>Cyclotella choctawhatcheeana</i>	OTU2226	/	/	/	/	0.020	0.023	0.018	0.020	JQ217341.1 (99.74%)
	s: unclassified-dinoflagellate	OTU2935	/	/	/	/	0.030	0.022	/	0.026	KY290715.1 (95.01%)

"/" indicates that the taxon was not a dominant species for a given sampling season. "g:" indicates a genus classification, while "s:" indicates a species-level classification.





areas (Figure 4). The Ace richness index did not significantly differ among areas in April, while the June culture area Ace index ( $201.4 \pm 18.4$ ) was significantly lower than that of the adjacent area ( $243.5 \pm 31.8$ ) ( $p < 0.05$ ).

### 3.4.2 Phytoplankton community beta diversity

Principal component analysis (PCA) was used to evaluate differences in phytoplankton community structure among all surface samples (Figure 5). Significant differences in phytoplankton community structure were observed among sampling areas in April ( $p = 0.010$ ), although significant differences were not observed in June ( $p = 0.088$ ) (Figure 5).

### 3.4.3 Correlation between dominant phytoplankton species and environmental factors

RDA analysis indicated that most dominant species abundances were positively correlated with metrics of N, P, and Si (except  $\text{NO}_2\text{-N}$ ) in April.  $\text{NO}_2\text{-N}$ , DO, and  $\text{PO}_4^{3-}\text{P}$  were the primary environmental factors associated with phytoplankton community structure in April. In addition, the abundances of dominant species were negatively correlated with nutrient values (except TN) in June, while TN and TP were the primary environmental factors associated with phytoplankton community structure (Figure 6).

The correlations between environmental factors ( $\text{NH}_4^+\text{-N}$ ,  $\text{NO}_2\text{-N}$ ,  $\text{NO}_3\text{-N}$ ,  $\text{PO}_4^{3-}\text{P}$ ,  $\text{SiO}_3^{2-}\text{Si}$ , TN, TP, DO PH, and Sal) and dominant phytoplankton species abundances in April were analyzed with phylogenetic molecular ecological networks (pMENs) (Figure 7).  $\text{NH}_4^+\text{-N}$  concentrations were significantly correlated with *Teleaulax amphioxeia* abundances ( $p < 0.05$ ), while  $\text{NO}_2\text{-N}$  concentrations were significantly correlated with *Ostreococcus* sp., *P. australis*, and *Minidiscus comicus* ( $p < 0.05$ ) in addition to *B. prasinos*, *M. pusilla*, and *Micromonas* sp. ( $p < 0.01$ ). In addition,  $\text{NO}_3\text{-N}$  concentrations were significantly correlated with *Storeatula major*, *M. comicus*, and *Thalassiosira rotula*

abundances ( $p < 0.05$ ), while TP was significantly correlated with *M. comicus* abundances ( $p < 0.05$ ). DO was significantly correlated with *Nannochloris* sp. abundances ( $p < 0.05$ ), while pH was significantly correlated with *Ostreococcus* sp., *Cryptomonas* sp., *Heterocapsa* sp., unclassified Dinophyta, *S. marinoi*, *T. tenera*, and *M. comicus* abundances ( $p < 0.05$ ).

The same analyses were conducted for environmental factors and dominant phytoplankton species in June communities (Figure 7). Again, TP levels were significantly correlated with unclassified Dinophyta abundances ( $p < 0.01$ ).  $\text{NO}_3\text{-N}$  concentrations were significantly correlated with *Cryptomonas* sp. and *Heterocapsa* sp. abundances ( $p < 0.05$ ), while DO concentrations were significantly correlated with unclassified Dinophyta abundances ( $p < 0.01$ ) in addition to those of *Cyclotella choctahatcheana*, *S. costatum*, *Minidiscus comicus*, and *T. tenera* ( $p < 0.05$ ). Lastly,  $\text{SiO}_3^{2-}\text{Si}$  concentrations were significantly correlated with unclassified Dinophyta abundances ( $p < 0.05$ ).

## 4 Discussion

### 4.1 Large-scale *S. fusiforme* cultivation could effectively increase marine carbon sequestration and helped mitigate coastal environmental problems

Large-scale *S. fusiforme* cultivation was associated with increased DO and pH in addition to decrease N within the cultivation area waters. Thus, *S. fusiforme* took up carbon (C), N, and P during photosynthesis and reduced N and P concentrations in seawater in addition to atmospheric carbon dioxide. These activities led to increase marine carbon sink capacity and DO levels that then increased water pH and helped preventing ocean acidification while also preventing eutrophication via efficient absorption of N and P along with other nutrients. Therefore, large-scale *S. fusiforme* cultivation

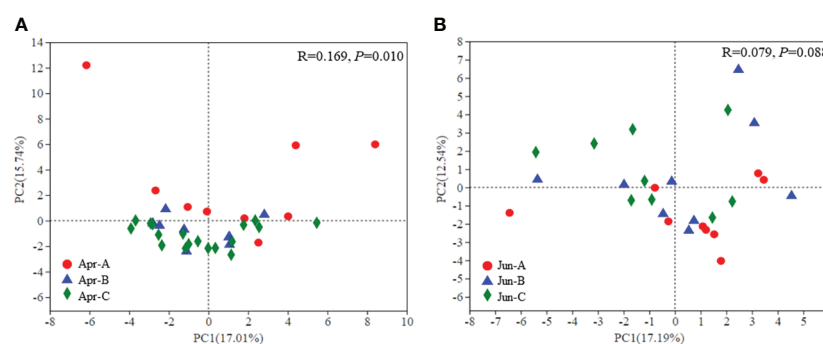
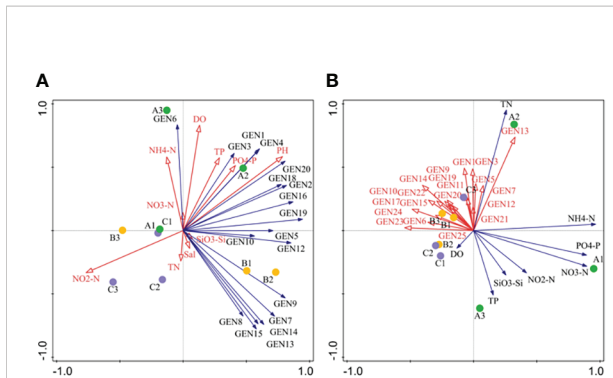


FIGURE 5  
 $\beta$ -diversity of phytoplankton community composition in April (A) and June (B) based on PCA ordinations.



**FIGURE 6** Redundancy analysis (RDA) of phytoplankton community composition based on high-throughput sequencing for April (A) and June (B) communities. Abbreviations are as follows: GEN1: *Bathycoccus prasinos*, GEN2: *Ostreococcus* sp., GEN3: *Micromonas pusilla*, GEN4: *Micromonas* sp., GEN5: *Pyramimonas australis*, GEN6: *Nannochloris* sp., GEN7: *Plagioselmis prolunga*, GEN8: *Teleaulexamphioxeia*, GEN9: *Cryptomonadales* sp., GEN10: *Storeatula major*, GEN11 *Teleaulex minuta*, GEN12: *Geminigera cryophila*, GEN13: *Heterocapsa* sp., GEN14: unclassified dinoflagellate, GEN15: *Gymnodinium* sp., GEN16: *Skeletonema marinoi*, GEN17: *Skeletonema costatum*, GEN18: *Thalassiosira rotula*, GEN19: *Thalassiosira tenera* GEN20: *Minidiscus comicus*, GEN21: *Cerataulina pelagica*, GEN22: *Chaetoceros tenuissimus*, GEN23: *Chaetoceros* sp., GEN24: *Cyclotella choctawcheeana*, and GEN25: unclassified dinoflagellate.

could effectively improve water quality and environmental characteristics, leading to beneficial habitat restoration effects. *S. fusiforme* might inhibit phytoplankton growth by reducing nutrient availability. The inhibited growth of phytoplankton living in shaded areas might be due to light shading effects by expanded seaweed thalli (Chai et al., 2018).

The dominant microalgae in the non-cultivation area waters in April were *B. prasinos*, *Geminigera cryophila*, *Heterocapsa* sp, *S.*

*marinoi*, and *Thalassiosira tenera*, but *B. prasinos*, *G. cryophila*, *H. sp.*, *S. costatum*, and *T. tenera* in June. We speculate that *S. fusiforme* inhibited the growth of the above species, leading to their dominance in non-cultivation waters. Consistent with this interpretation, seawater extracts of hijiki dry powder contains substances that inhibit *S. costatum*, wherein the inhibitory effect increases with extract concentrations, suggesting that inhibitory substances in the extracts were presumably secondary metabolites with allelopathic effects (Zhang et al., 2021).

In this study there was no significant difference in the relative abundance of the dominant species *Heterocapsa* sp., *P. prolunga*, and *B. prasinos* among the sampling areas in April. Therefore, the dominant phyla of phytoplankton in the coastal ocean would not change due to the cultivation of *S. fusiforme*. The observed differences in community structure between April and June indicated a seasonal influence on communities that was consistent with other studies showing such trends due to seasonal variation of environmental factors such as temperature and nutrients (Chen et al., 2016; Lamont et al., 2018).

Significant differences between areas with and without *S. fusiforme* cultivation were observed when comparing several estimates of phytoplankton  $\alpha$  and  $\beta$  biodiversity based on high-throughput sequencing approaches. Thus, these results pointed to a critical ecological significance of *S. fusiforme* cultivation, since biodiversity is one of the most important indicators of coastal ecosystem health and forms the basis of ecosystem productivity (Cardinale et al., 2012; Fraser et al., 2015; Isbell et al., 2015). Specifically, the results of this study indicated that large-scale cultivation of *S. fusiforme* maintained or enhanced phytoplankton community biodiversity via nutrient and light competition between seaweeds and phytoplankton. Therefore, these results demonstrated that large-scale cultivation of *S. fusiforme* could provide raw materials with high edible, medicinal, and industrial

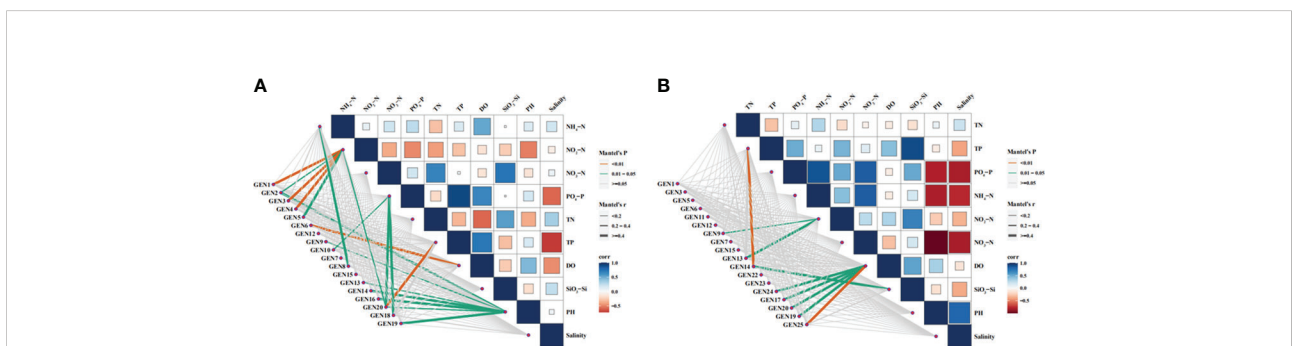


**FIGURE 7** Relationships between environmental factors and the abundances of dominant phytoplankton species based on phylogenetic molecular ecological network analysis. Abbreviations are as follows: GEN1: *Bathycoccus prasinos*, GEN2: *Ostreococcus* sp., GEN3 *Micromonas pusilla*, GEN4: *Micromonas* sp., GEN5: *Pyramimonas australis*, GEN6: *Nannochloris* sp., GEN7: *Plagioselmis prolunga*, GEN8: *Teleaulex amphioxeia*, GEN9: *Cryptomonadales* sp., GEN10: *Storeatula major*, GEN11: *Teleaulex minuta*, GEN12: *Geminigera cryophila*, GEN13: *Heterocapsa* sp., GEN14: unclassified dinoflagellate, GEN15: *Gymnodinium* sp., GEN16: *Skeletonema marinoi*, GEN17: *Skeletonema costatum*, GEN18: *Thalassiosira rotula*, GEN19: *Thalassiosira tenera* GEN20: *Minidiscus comicus*, GEN21: *Cerataulina pelagica*, GEN22: *Chaetoceros tenuissimus*, GEN23: *Chaetoceros* sp., GEN24: *Cyclotella choctawhatcheeana*, and GEN 25: unclassified dinoflagellate.

value and thus represented a promising strategy for controlling harmful algal blooms and eutrophication.

## 4.2 High-throughput sequencing provided more accurate microplankton identification

A total of 75 phytoplankton species were identified based on morphology, while a parallel survey of phytoplankton communities using high-throughput cultivation-independent sequencing identified 601 phytoplankton OTUs. Thus, the number of OTUs in this study was 3 to 7.6 times higher than the number of morphospecies identified from the same communities. This difference was likely attributable the high morphological similarity of species based on current taxonomy. For example, *Skeletonema* was one of the most abundant genera of phytoplankton observed in this study, comprising the five species *S. marinoi*, *S. costatum*, *S. potamos*, *S. menzelleri*, and *S. subsalsum* based on high-throughput sequencing. In contrast, only *S. costatum* was identified based on traditional morphological observations due to high similarity in morphological appearance. In addition, the smallest known eukaryotes (~ 1 mm diameter cell sizes) (Chai et al., 2018) were observed for the first time in the study area. The actual number of phytoplankton species should be lower than those indicated by DNA sequencing approaches (Qiao et al., 2020). However, these higher OTU numbers likely reflected the genetic diversity among many morphospecies, and possibly the presence of some cryptic species or species complexes (Chai et al., 2018).

Phytoplankton communities detected with high-throughput sequencing are strikingly more diverse than those determined by microscopic detection, as many species exhibit relatively small sizes or are morphologically simple or similar to others (Liu et al., 2022). Furthermore, dormant cells, dead cells, or even cell fragments can be identified and lead to spurious diversity or abundance estimates (Santoferrara et al., 2020; Eliáš, 2021; Burki et al., 2021; Liu et al., 2022). Previous investigations of phytoplankton composition and diversity have primarily relied on traditional optical microscopy (Soares et al., 2011) that relies on cell morphological identification, rendering it difficult to recognize and distinguish similar taxa (Qiao et al., 2020). In this study, 21 species of nanophytoplankton accounted for 22.21% of the total sequences, while 17 species of picophytoplankton accounted for 13.18% of the total sequences from high-throughput sequencing, and these taxa were not observed using morphological analysis. Dominant Chlorophyta species such as *B. prasinos*, *M. pusilla*, *P. australis*, and *Picochlorum* sp. that are less than 2 µm in diameter are PPEs that are widely distributed in marine environments (Mayer and Taylo, 1979; Luis et al., 1992; Rashid et al., 2018). However, it was impossible to observe the above species by morphological observation; consequently, the use of high-throughput sequencing was necessary to comprehensively

assess the diversity and community structure of phytoplankton. This will generally lead to higher biodiversity estimates.

## 4.3 The effects of *S. fusiforme* on phytoplankton community structure

RDA analysis indicated that DO, PO<sub>4</sub><sup>3-</sup>-P, and NH<sub>4</sub><sup>+</sup>-N were the main environmental factors affecting phytoplankton community structure in April among the factors measured, while DO levels in the culture area were significantly higher than in adjacent and control areas. The latter was primarily due to the photosynthetic oxygen release of *S. fusiforme*, and thus the effect of DO on phytoplankton community structure could be attributed to the effects of *S. fusiforme* on the phytoplankton community structure. A positive correlation was observed between phytoplankton community structure and nutrient concentrations, suggesting that seawater nutrients were consumed by *S. fusiforme*, thereby limiting phytoplankton growth to a certain extent. Consequently, *S. fusiforme* appeared to play a key role in regulating phytoplankton growth.

## 5 Conclusions

In summary, the results of the present study indicated that large-scale cultivation of *S. fusiforme* could reduce N and P concentrations in seawater, thereby helping to prevent eutrophication. Moreover, cultivation could increase water DO levels that could also help reduce the adverse effects of hypoxia while increasing water pH to prevent ocean acidification. In addition, large-scale cultivation of *S. fusiforme* played an important role in stabilizing phytoplankton community structure by improving phytoplankton diversity via the inhibition of harmful algal growth, potentially through allelopathy, nutrient competition and shading. Consequently, this study demonstrated that large-scale cultivation of *S. fusiforme* in coastal regions was an effective approach for increasing marine carbon sink capacities and helping to solve environmental problems in marine ecosystems.

## Data availability statement

The datasets presented in this study can be found in online repositories. The names of the repository/repositories and accession number(s) can be found below: <https://www.ncbi.nlm.nih.gov/>, PRJNA761497

## Author contributions

YZ: Conceptualization, Methodology, Software, Writing-original draft, Funding acquisition. DX: Supervision, Project

administration, Validation, Writing - review and editing. TL: Investigation, Methodology, Validation. LQ: Investigation, Methodology, Validation. NX: Resources, Validation, Supervision, Writing - review and editing, Funding acquisition. All authors contributed to the article and approved the submitted version.

## Funding

This work was supported by the National Key R&D Program of China (grant numbers: 2018YFD0900702) and the Natural Science Foundation of Zhejiang Province (LZ17D060001 and LGF19D060002)

## References

- Alonso-González, A., Orive, E., David, H., Garcia-Etxebarria, K., Luis Garrido, J., Laza-Martinez, A., et al. (2014). Scaly green flagellates from Spanish Atlantic coastal waters: molecular, ultrastructural and pigment analyses. *Bot. Mar.* 57 (5), 379–402. doi: 10.1515/bot-2013-0108
- Antoni, J. S., Almandoz, G. O., Ferrario, M. E., Hernando, M. P., Varel, D. E., Rozem, P. D, et al (2020). Response of a natural Antarctic phytoplankton assemblage to changes in temperature and salinity. *J. Exp. Mar. Biol. Ecol.* 532, 151444. doi: 10.1016/j.jembe.2020.151444
- Augustine, A., Kumaran, J., Puthumana, J., Sabu, S., and Singh, B. I. S. (2017). Multifactorial interactions and optimization in biomass harvesting of marine picoalga *Picochlorum maculatum* MACC3 with different flocculants. *Aquaculture* 474, 18–25. doi: 10.1016/j.aquaculture.2017.03.020
- Behrenfeld, M. J., O'Malley, R. T., Siegel, D. A., and McClain, C. R. (2006). Climate-driven trends in contemporary ocean productivity. *Nature* 444 (7120), 752–755. doi: 10.1038/nature05317
- Bock, C., Luo, W., Kusber, W. H., Hegewald, E., Pažoutová, M., and Krienitz, L. (2013). Classification of crucigenoid algae: phylogenetic position of the reinstated genus *Lemmertmannia*, tetrastrum spp. *Crucigenia tetrapedia*, and *C. lauterbornii* (Trebouxiophyceae, chlorophyta) (1). *J. Phycol.* 49 (2), 329–339. doi: 10.1111/jpy.12039
- Burki, F., Sandin, M. M., and Jamy, M. (2021). Diversity and ecology of protists revealed by metabarcoding. *Curr. Biol.* 31 (19), R1267–R1280. doi: 10.1016/j.cub.2021.07.066
- Caporaso, J. G., Kuczynski, J., and Stombaugh, J. (2010). QIIME allows analysis of high-throughput community sequencing data. *Nat. Methods* 7, 335–336. doi: 10.1038/nmeth.f.303
- Cardinale, B. J., Duffy, J. E., Gonzalez, A., Hooper, D. U., Perrings, C., Venail, P., et al. (2012). Biodiversity loss and its impact on humanity. *Nature* 486, 59–67. doi: 10.1038/nature11148
- Chai, Z. Y., He, Z. L., Yun, Y., Yang, Y. F., and Tang, Y. Z. (2018). Cultivation of seaweed *Gracilaria lemaneiformis* enhanced biodiversity in an eukaryotic plankton community as revealed via metagenomic analyses. *Mol. Ecol.* 27, 1081–1093. doi: 10.1111/mec.14496
- Chen, Y., Gao, Y., Chen, C., Liang, J., and Sun, L. (2016). Seasonal variations of phytoplankton assemblages and its relation to environmental variables in a scallop culture sea area of bohai bay, China, mar. *pollut. Bull.* 113 (1–2), 362–370. doi: 10.1016/j.marpolbul.2016.10.025
- Chen, B., Zou, D., Ma, Z., Yu, P., and Wu, M. (2018). Effects of light intensity on the photosynthetic responses of *Sargassum fusiforme* seedlings to future CO<sub>2</sub> rising. *Aquac. Res.* 50, 116–125. doi: 10.1111/arc.13873
- Christiane, S. (2003). *Cylotella choctawbatcheanae* häufige diatomee aus sedimenthorizonten und einer wasserprobe des Greifswalder boddens(südliche ostsee). *Senckenbe. Marit.* 32, 35–50. doi: 10.1007/BF03043084
- de Vargas, C., Audic, S., Henry, N., Decelle, J., Mahe, F., Logares, R., et al. (2015). Eukaryotic plankton diversity in the sunlit ocean. *Science* 348, 1261605. doi: 10.1126/science.1261605
- Dunthorn, M., Klier, J., Bunge, J., and Stoeck, T. (2012). Comparing the hyper-variable V4 and V9 regions of the small subunit rDNA for assessment of ciliate environmental diversity. *J. Eukaryot. Microbio.* 59 (2), 185–187. doi: 10.1111/j.1550-7408.2011.00602.x
- Elge, E. S., Johannessen, T. V., Andersen, T., Eikrem, W., Bittner, L., Larsen, A., et al. (2015). Seasonal diversity and dynamics of haptophytes in the skagerrak, Norway, explored by high-throughput sequencing. *Mol. Ecol.* 24, 3026–3042. doi: 10.1111/mec.13160
- Eliáš, M. (2021). Protist diversity: novel groups enrich the algal tree of life. *Curr. Biol.* 31 (11), R733–R735. doi: 10.1016/j.cub.2021.04.025
- Emerson, S. (2014). Annual net community production and the biological carbon flux in the ocean. *Global Biogeochem. Cy.* 28 (1), 14–28. doi: 10.1002/2013GB004680
- Falkowski, P., Scholes, R. J., Boyle, E. E. A., Canadell, J., Canfield, D., Elser, J., et al. (2000). The global carbon cycle: a test of our knowledge of earth as a system. *Science* 290 (5490), 291–296. doi: 10.1126/science.290.5490.291
- Fraser, L. H., Pither, J., Jentsch, A., Sternberg, M., Zobel, M., Askarizadeh, D., et al. (2015). Worldwide evidence of a unimodal relationship between productivity and plant species richness. *Science* 349, 302–305. doi: 10.1126/science.aab3916
- Handelsman, J., Rondon, M. R., Brady, S. F., Clardy, J., and Goodman, R. M. (1998). Molecular biological access to the chemistry of unknown soil microbes: a new frontier for natural products. *Chem. Bio.* 5 (10), R245–R249. doi: 10.1016/S1074-5521(98)90108-9
- Hiroshi, S., Mayumi, M., Takeshi, N., and Isao, I. (2002). Vestigial chloroplasts in heterotrophic stramenopiles pteridomonas danica and *Ciliophrys infusioformis* (Dictyochophyceae). *Protist* 153, 157–167. doi: 10.1078/1434-4610-00094
- Howe, A. T., Bass, D. J., Scoble, J. M., et al. (2011). Novel Cultured Protists Identify Deep-branching Environmental DNA Clades of Cercozoa: New Genera Tremula, Micrometopion, Minimassteria, Nudifila, Peregrinia. *Protist* 162, 332–72. doi: 10.1016/j.protis.2010.10.002
- Ichinomiya, M., Yamada, K., Nakagawa, Y., Nishino, Y., Kasai, H., and Kuwata, A. (2019). Parmales abundance and species composition in the waters surrounding Hokkaido, north Japan. *Polar Sci.* 9, 130–136. doi: 10.1016/j.polar.2018.08.001
- Isbell, F., Craven, D., Connolly, J., Loreau, M., Schmid, B., Beierkuhnlein, C., et al. (2015). Biodiversity increases the resistance of ecosystem productivity to climate extremes. *Nature* 526, 574–577. doi: 10.1038/nature15374
- Jardillier, L., Zubkov, M. V., Pearman, J., and Scanlan, D. J. (2010). Significant CO<sub>2</sub> fixation by small prymnesiophytes in the subtropical and tropical northeast Atlantic ocean. *ISME J.* 4 (9), 1180–1192. doi: 10.1038/ismej.2010.36
- Jouenne, F., Eikrema, W., Le Gall, F., Marie, D., Johnsen, G., and Vault, D. (2011). *Prasinoderma singularis* sp. nov. (Prasinophyceae, chlorophyta), a solitary coccoid prasinophyte from the south-East pacific ocean. *Protist* 162, 70–84. doi: 10.1016/j.protis.2010.04.005
- Kagan, M. L., and Matulka, R. A. (2015). Safety assessment of the microalgae *Nannochloropsis oculata*. *Toxicol. Rep.* 2, 617–623. doi: 10.1016/j.toxrep.2015.03.008
- Lamont, T., Brewin, R. J. W., and Barlow, R. G. (2018). Seasonal variation in remotely-sensed phytoplankton size structure around southern Africa. *Remote Sens. Environ.* 204, 617–631. doi: 10.1016/j.rse.2017.09.038
- Leblad, B. R., Amnhir, R., Requia, S., Sittel, F., and Daoudi, M. (2020). Seasonal variations of phytoplankton assemblages in relation to environmental factors in Mediterranean coastal waters of Morocco, a focus on HABs species. *Harmful Algae* 96, 101819. doi: 10.1016/j.hal.2020.101819
- Leblanc, K., Quéguiner, B., Diaz, F., and Michel-Rodriguez, M. (2018). Nanoplanktonic diatoms are globally overlooked but play a role in spring

## Conflict of interest

The authors declare that they have no known competing financial interests or personal relationships that could have appeared to influence the work reported in this paper.

## Publisher's note

All claims expressed in this article are solely those of the authors and do not necessarily represent those of their affiliated organizations, or those of the publisher, the editors and the reviewers. Any product that may be evaluated in this article, or claim that may be made by its manufacturer, is not guaranteed or endorsed by the publisher.

- blooms and carbon export. *Nat. Commun.* 9, 953. doi: 10.1038/s41467-018-03376-9
- Lee, S. R., Oak, J. H., Chung, I. K., and Lee, J. A. (2010). Effective molecular examination of eukaryotic plankton species diversity in environmental seawater using environmental PCR, PCR-RFLP, and sequencing. *J. Appl. Phycol.* 22, 699–707. doi: 10.1007/s10811-010-9509-7
- Lefebvre, S., Lawson, T., Fryer, M., Zakhleniuk, O. V., Lloyd, J. C., and Raines, C. A. (2005). Increased sedoheptulose-1,7-bisphosphatase activity in transgenic tobacco plants stimulates photosynthesis and growth from an early stage in development. *Plant Physiol.* 138 (1), 451–460.
- Li, J., Li, J., Liu, Y., Liu, Y., Wang, Q., Gao, X., et al. (2019). Effects of temperature and salinity on the growth and biochemical composition of the brown alga *Sargassum fusiforme* (Fucales, phaeophyceae). *J. Appl. Phycol.* 31, 3061–3068. doi: 10.1007/s10811-019-01795-9
- Lincoln, AM, Kirsty, FS, Lesley, LR, et al (2011). Mortalities of sea-cage salmon (*Oncorhynchus tshawytscha*) due to a bloom of *Pseudochattonella verruculosa* (Dictyochophyceae) in Queen Charlotte Sound, New Zealand. *Harmful Algae* 11, 45–53. doi: 10.1016/j.hal.2011.07.003
- Liu, S., Gibson, K., Cui, Z., Chen, Y., Sun, X., and Chen, N. (2020a). Metabarcoding analysis of harmful algal species in jiaozhou bay. *Harmful Algae* 92. doi: 10.1016/j.hal.2020.101772
- Liu, J., Ling, S., Chen, Q., Shen, Y., and Zhang, J. (2020). Different extraction methods bring about distinct physicochemical properties and antioxidant activities of *Sargassum fusiforme* fucoidans. *Int. J. Bio.Macromol.* 155, 1385–1392. doi: 10.1016/j.ijbiomac.2019.11.113
- Liu, W., Song, L., and Wu, J. (2017). Optimization of high-throughput sequencing primers for nanophytoplankton and picophytoplankton in environmental samples. *Acta Ecol. Sin.* 37 (12), 4208–4216. doi: 10.5846/stxb201605180963
- Luis, M. L., Julián, B., and Rafael, E. (1992). A comparative study of acid and alkaline phosphatase activities in several strains of *nannochloris* (Chlorophyceae) and *nannochloropsis* (Eustigmatophyceae), br. *Phycol. J.* 27, 119–130. doi: 10.1080/00071619200650131
- Mackenzie, L. A., Smith, K. F., and Rhodes, L. L. (2011). Mortalities of sea-cage salmon (*Oncorhynchus tshawytscha*) due to a bloom of *pseudochattonella verruculosa* (dictyochophyceae) in queen charlotte sound, new zealand. *Harmful Algae* 11, 41–53. doi: 10.1016/j.hal.2011.07.003
- Malviya, S., Scalco, E., Audic, S., Vincent, F., and Veluchamy, A. (2016). Insights into global diatom distribution and diversity in the world's ocean. *PNAS* 113(11), E1516–E1525. doi: 10.1073/pnas.1509523113
- Manoylov, K. M. (2014). Taxonomic identification of algae (morphological and molecular): species concepts, methodologies, and their implications for ecological bioassessment. *J. Phycol.* 50 (3), 409–424. doi: 10.1111/jpy.12183
- Massana, R. (2011). Eukaryotic picoplankton in surface oceans. *Annu. Rev. Microbiol.* 65, 91–110. doi: 10.1146/annurev-micro-090110-102903
- Ma, Z., Wu, M., Lin, L., Ronald, W. T., Yu, H., and Zhang, X. (2017). Allelopathic interactions between the macroalga *Hizikia fusiformis* (Harvey) and the harmful blooms-forming dinoflagellate *Karenia mikimotoi*. *Harmful Algae* 65, 19–26. doi: 10.1016/j.hal.2017.04.003
- Mayer, J. A., and Taylo, F. J. R. (1979). A virus which lyses the marine nanoflagellate *Micromonas pusilla*. *Nature* 281, 299–301. doi: 10.1038/281299a0
- Moro, I., La Rocca, N., Dalla Valle, L., Moschin, E., Negrisol, E., and Andreoli, C. (2002). *Pyramimonas australis* sp. nov. (Prasinophyceae, chlorophyta) from Antarctica: fine structure and molecular phylogeny. *Eur. J. Phycol.* 37, 103–114. doi: 10.1017/S0967026201003493
- Navas-Parejo, J. C. C., Corzoa, A., and Papispyroua, S. (2020). Seasonal cycles of phytoplankton biomass and primary production in a tropical temporarily open-closed estuarine lagoon—the effect of an extreme climatic event. *Sci. Total Environ.* 723, 138014. doi: 10.1016/j.scitotenv.2020.138014
- Neefs, J. M., Van de Peer, Y., Hendriks, L., and De Wachter, R. (1990). Compilation of small ribosomal subunit RNA sequences. *Nucleic Acids Res.* 18 (Suppl), 2237–2317. doi: 10.1093/nar/18.suppl.2237
- Nozaki, H. (2003). “Flagellated green algae,” in *Freshwater algae of north America: Ecology and classification*. Academic Press/Eds. J. D. Wehr and R. G. Sheath (Elsterdam), 225–252.
- Parsons, M. L., Brandt, A. L., Turner, R. E., Morrison, W. L., and Rabalais, N. N. (2021). Characterization of common phytoplankton on the Louisiana shelf. *Mari. Pollut. Bull.* 168, 112458. doi: 10.1016/j.marpolbul.2021.112458
- Pawlowski, J., Christen, R., Lecroq, B., Bachar, D., Shahbazkia, H. R., Amaral-Zettler, L., et al. (2011). Eukaryotic richness in the abyss: insights from pyrotag sequencing. *PLoS One* 6 (4), e18169. doi: 10.1371/journal.pone.0018169
- Peng, X., Zhang, L., Li, Y., Lin, Q., and He, C. (2021). The changing characteristics of phytoplankton community and biomass in subtropical shallow lakes: Coupling effects of land use patterns and lake morphology. *Water Res.* 200, 117235. doi: 10.1016/j.watres.2021.117235
- Pfannkuchen, D. M., Godrijan, J., Tankovic, M. S., Baricevic, A., Kuzat, N., Djakovac, T., et al. (2018). The ecology of one cosmopolitan, one newly introduced and one occasionally advected species from the genus *skeletonema* in a highly structured ecosystem, the northern Adriatic. *Microb. Ecol.* 75, 674–687. doi: 10.1007/s00248-017-1069-9
- Qiao, L., Chang, Z., Li, J., and Chen, Z. (2020). Phytoplankton community succession in relation to water quality changes in the indoor industrial aquaculture system for *litopenaeus vannamei*. *Aquaculture* 527, 735441. doi: 10.1016/j.aquaculture.2020.735441
- Rashid, J., Kobiyama, A., Reza, M. S., Yamada, Y., and Ikeda, Y. (2018). Seasonal changes in the communities of photosynthetic picoeukaryotes in ofunato bay as revealed by shotgun metagenomic sequencing. *Gene* 665, 127–132. doi: 10.1016/j.gene.2018.04.071
- Samanta, B., Kinney, M. E., Heffell, Q., Ehrman, J. M., and Kaczmarek, I. (2017). Gametogenesis and auxospore development in the bipolar centric diatom *brockmanniella brockmannii* (Family cymatosiraceae). *Protist* 168, 527–545. doi: 10.1016/j.protis.2017.07.004
- Santoferrara, L., Burki, F., Filker, S., Logares, R., Dunthorn, M., and McManus, G. B. (2020). Perspectives from ten years of protist studies by high-throughput metabarcoding. *J. Eukaryot. Microbiol.* 67 (5), 612–622. doi: 10.1111/jeu.12813
- Shan, K., Song, L. R., Chen, W., Li, L., Liu, L. M., and Wu, Y. L. (2019). Analysis of environmental drivers influencing interspecific variations and associations among bloom-forming cyanobacteria in large, shallow eutrophic lakes. *Harmful Algae* 84, 84–94. doi: 10.1016/j.hal.2019.02.002
- Sieburth, J. M., Johnson, P. W., and Hargraves, P. E. (1985). Ultrastructure and ecology of *aureococcus anophage-ferrens* gen. et sp. nov. (Chrysophyceae) the dominant picoplankton during a bloom in Narragansett bay, Rhode island, summer. *J. Phycol.* 24, 416–425. doi: 10.1111/j.1529-8817.1988.tb04485.x
- Simon, N., Fouloua, E., Grulois, D., Christophe, S., and Yves, D. (2017). Revision of the genus *micromonas* Manton et parke (Chlorophyta, mamiellophyceae), of the type species *m. pusilla* (Butcher) Manton et parke and of the species *M. commoda* van baren, bachy and worden and description of two new species based on the genetic and phenotypic characterization of cultured isolates. *Protist* 168, 612–635. doi: 10.1016/j.protis.2017.09.002
- Sivakumar, G., Jeong, K., and Lay, J. O. (2014). Bioprocessing of *Stichococcus bacillaris* strain siva2011. *Biotechnol. Biofuels* 7, 62. doi: 10.1186/1754-6834-7-62
- Soares, M. C., Lobao, L. M., Vidal, L. O., Noyma, N. P., Barros, N. O., and Cardoso, S. J. (2011). Light microscopy in aquatic ecology: methods for plankton communities studies. *Methods Mol. Biol.* 689, 215–227. doi: 10.1007/978-1-60761-950-5\_13
- Song, L., Wu, J., and Song, G. J. (2020). High-throughput sequencing and comparative analysis of eukaryotic phytoplankton community in liaodong bay, China. *Reg. Stud. Mar. Sci.* 40, 10150. doi: 10.1016/j.rsma.2020.101508
- Stoeck, T., Bass, D., Nebel, M., Christen, R., Jones, M. D., and Breiner, H. W. (2010). Multiple marker parallel tag environmental DNA sequencing reveals a highly complex eukaryotic community in marine anoxic water. *Mol. Ecol.* 19, 21–31. doi: 10.1111/j.1365-294X.2009.04480.x
- Tomaru, Y., Toyoda, K., and Kimura, K. (2018). Occurrence of the planktonic bloom-forming marine diatom *Chaetoceros tenuissimus* meunier and its infectious viruses in western Japan. *Hydrobiologia* 805, 221–223. doi: 10.1007/s10750-017-3306-0
- Vaulot, D., Eikrem, W., Viprey, M., and Moreau, H. (2008). The diversity of small eukaryotic phytoplankton (3µm) in marine ecosystems. *Fems. Microbiol. Rev.* 32, 795–820. doi: 10.1111/j.1574-6976.2008.00121.x
- Xing, X., Lin, X., Chen, C., Gao, Y., and Liang, J. (2008). Observations of several cryptomonad flagellates from China Sea by scanning electron microscopy. *J. Syst. Evo.* 46 (2), 205–212. doi: 10.3724/SP.J.1002.2008.07073
- Zhang, F., He, J., Lin, L., and Jin, L. (2015). Dominance of picophytoplankton in the newly open surface water of the central Arctic ocean. *Polar Biol.* 38 (7), 1081–1089. doi: 10.1007/s00300-015-1662-7
- Zhang, Z., Liu, J., and Liu, J. (2002). Study review of *Hizikia fusiformis*. *mar. fishe. Res.* 23, 67–74.
- Zhang, Y., Xu, N., Li, H., and Li, Z. (2021). Evaluation of the correlation of *Sargassum fusiforme* cultivation and biodiversity and network structure of marine bacteria in the coastal waters of dongtuo island of China. *Aquaculture* 2021, 737057. doi: 10.1016/j.aquaculture.2021.737057
- Zhang, R., Zhang, X., Tang, Y., and Mao, J. (2020). Composition, isolation, purification and biological activities of *sargassum fusiforme* polysaccharides: A review. *carbohydr. Polym.* 228, 115381. doi: 10.1016/j.carbpol.2019.115381
- Zhang, X., Zhou, H., and Zhang, H. (2006). The effect of *Sargassum fusiforme* polysaccharide extracts on vibriosis resistance and immune activity of the shrimp, *fenneropenaeus chinensis*. *Fish Shellfish Immunol.* 20, 750–757. doi: 10.1016/j.fsi.2005.09.008
- Zhou, Y., Yang, X., Wang, Y., Li, F., Wang, J., and Tan, L. (2021). Exogenous nutrient inputs restructure phytoplankton community and ecological stoichiometry of Eastern Indian ocean. *Ecol. Indic.* 127, 107801. doi: 10.1016/j.ecolind.2021.107801